
HYPERBOLIC GRAPH NEURAL NETWORKS: A REVIEW OF METHODS AND APPLICATIONS

Menglin Yang^{1*}, Min Zhou^{2*}, Zhihao Li³, Jiahong Liu³, Lujia Pan², Hui Xiong⁴ and Iriwn King¹

¹The Chinese University of Hong Kong, Hong Kong, China

²Huawei Noah's Ark Lab, Shenzhen, China

³Harbin Institute of Technology, Shenzhen, China

⁴Hong Kong University of Science and Technology, Guangzhou, China

^{*}Correspondence to: mlyang@link.cuhk.edu.hk; zhoumin27@huawei.com

ABSTRACT

Graph neural networks generalize conventional neural networks for graph-structured data and have garnered widespread attention because of their impressive representation capability. Despite these significant achievements, the performance of Euclidean models in graph-related learning remains constrained by the representational capacity of Euclidean geometry, particularly for datasets exhibiting a highly non-Euclidean latent anatomy. Recently, hyperbolic spaces have grown in popularity for processing graph data with tree-like structures or power-law distributions, thanks to their exponential growth property. In this survey, we provide a comprehensive review of the current hyperbolic graph neural networks¹, integrating them into a unified framework and detailing the variations of each component. Moreover, we highlight a series of pertinent applications across diverse fields. Most importantly, we pinpoint several challenges that could serve as directives for further enhancing the accomplishments of graph learning in hyperbolic spaces.

Keywords Hyperbolic geometry · Graph neural network · Graph representation learning

1 Introduction

Graphs are data structures that extensively exist in real-world complex systems, varying from social networks [15, 62], protein interaction networks [52], recommender systems [9, 65, 64], knowledge graphs [56], to the financial transaction systems [40]. They form the basis of innumerable systems owing to their widespread utilization, allowing relational knowledge about interacting entities to be stored and accessible rapidly. Consequently, graph-related learning tasks gain increasing attention in machine learning and network science research. Many researchers have applied Graph Neural Networks (GNNs) for a variety of tasks, including node classification [23, 53, 59], link prediction [22, 71], and graph classification [61, 11] by embedding nodes in low-dimensional vector spaces, encoding topological and semantic information simultaneously. Many GNNs are built in Euclidean space in that it feature a vectorial structure, closed-form distance and inner-product formulae and is a natural extension of our intuitively appealing visual three-dimensional space [14].

Despite the effectiveness of Euclidean space for graph-related learning tasks, its ability to encode complex patterns is intrinsically limited by its polynomially expanding capacity. Although nonlinear techniques [3] assist in mitigating this issue, complex graph patterns may still need an embedding dimensionality that is computationally intractable. As revealed by recent research [4] many complex data show non-Euclidean underlying anatomy. For example, the tree-like structure extensively exists in many real-world networks, such as the hypernym structure in natural languages, the subordinate structure of entities in the knowledge graph, the organizational structure for financial fraud, and the power-law distribution in recommender systems.² In these situations, Euclidean space fails to make the most powerful or adequate geometrical representations.

¹<https://github.com/marlin-codes/HGNNs>

²The power-law distribution can be traced back to the hierarchical structures [39].

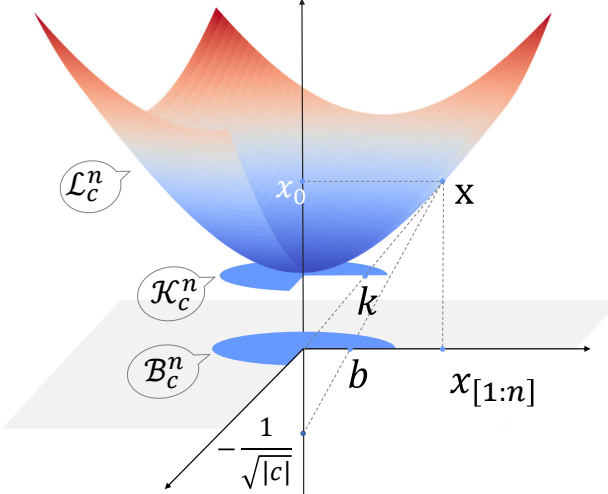


Figure 1: Illustration of three prevalent and isomorphic hyperbolic graph models: Lorentz model, Kelin model, and Poincaré ball model.

Recently, hyperbolic space has gained increasing popularity in processing tree-like graph data. Figure 1 depicts three prevalent models for hyperbolic space, and they are isomorphic. The typical geometric property of hyperbolic space is that its volume increases exponentially in proportion to its radius, whereas Euclidean space grows polynomially. Such a geometric trait brings two benefits, enabling it to deal well with tree-like graph data. The *first* one is that hyperbolic space exhibits minimal distortion and fits the hierarchies particularly well since the space closely matches the growth rate of tree-like data while the Euclidean space cannot. The *second* is that even though with a low-embedding dimension space, hyperbolic models are surprisingly able to produce a high-quality representation, which makes it especially favorable in low-memory and low-storage scenarios.

Scope and Structure of the Survey. To the best of our knowledge, no surveys have been conducted mainly on the methods and applications of Hyperbolic Graph Neural Networks (HGNNs), and the most recent relevant study [37] mainly sketches the progress of hyperbolic neural networks without focusing on the latest methods and applications in graph field. In this work, we attempt to fill this gap by scoping the latest research efforts on HGNNs. The main contributions of this work are summarized below:

- We provide a detailed technique review over existing HGNN models, unifying them by a general framework and outlining the variants of each module. Additionally, we discuss recent studies on theoretical and empirical analysis of HGNN models.
- We systematically categorize the applications and divide them into numerous scenarios. For each case, we present several major applications and their corresponding methods.
- We summarize several challenges and opportunities for future research, providing insights for further flourishing the achievements of graph learning built with hyperbolic spaces.

2 Preliminaries and Notation

In this section, we briefly introduce a list of some of the most helpful Riemannian geometry concepts, definitions, and operations in hyperbolic geometry. For a more detailed introduction, please refer to [25] and [26].

Manifold and Tangent Space. Riemannian geometry is a sub-field of differential geometry in which a smooth manifold \mathcal{M} is associated with a Riemannian metric $g^{\mathcal{M}}$. An n -dimensional manifold $(\mathcal{M}, g^{\mathcal{M}})$ is a topological space, a generalization of a 2-dimensional surface with high dimensions. For each point \mathbf{x} in \mathcal{M} , a tangent space $T_{\mathbf{x}}\mathcal{M}$ is defined as the first-order approximation of \mathcal{M} around \mathbf{x} , which is an n -dimension vector space and isomorphic to \mathbb{R}^n . The Riemannian manifold metric $g^{\mathcal{M}}$ assigns a smoothly varying positive definite inner product $\langle \cdot, \cdot \rangle: T_{\mathbf{x}}\mathcal{M} \times T_{\mathbf{x}}\mathcal{M} \rightarrow \mathbb{R}$ on the tangent space, which allows us to define several geometric properties, such as geodesic distances, angles, and curvature.

Table 1: Summary of operations in the Poincaré ball model and the Lorentz model ($c < 0$)

	Poincaré Ball Model	Lorentz Model
Manifold	$\mathcal{B}_c^n = \{x \in \mathbb{R}^n : \langle x, x \rangle_2 < -1/c\}$	$\mathcal{L}_c^n = \{x \in \mathbb{R}^{n+1} : \langle x, x \rangle_{\mathcal{L}} = 1/c\}$
Metric	$g_x^{\mathcal{B}} = (\lambda_x^c)^2 g^E$ where $\lambda_x^c = \frac{2}{1+c\ x\ _2^2}$ and $g^E = \mathbf{I}_n$	$g_x^{\mathcal{L}} = \eta$, where η is I except $\eta_{0,0} = -1$
Induced distance	$d_{\mathcal{B}}^c(x, y) = \frac{1}{\sqrt{ c }} \cosh^{-1} \left(1 - \frac{2c\ x-y\ _2^2}{(1+c\ x\ _2^2)(1+c\ y\ _2^2)} \right)$	$d_{\mathcal{L}}^c(x, y) = \frac{1}{\sqrt{ c }} \cosh^{-1} (c \langle x, y \rangle_{\mathcal{L}})$
Logarithmic map	$\log_x^c(y) = \frac{2}{\sqrt{ c }\lambda_x^c} \tanh^{-1} \left(\sqrt{ c } \ -x \oplus_c y \ _2 \right) \frac{-x \oplus_c y}{\ -x \oplus_c y \ _2}$	$\log_x^c(y) = \frac{\cosh^{-1}(c \langle x, y \rangle_{\mathcal{L}})}{\sinh(\cosh^{-1}(c \langle x, y \rangle_{\mathcal{L}}))} (y - c \langle x, y \rangle_{\mathcal{L}} x)$
Exponential map	$\exp_x^c(v) = x \oplus_c \left(\tanh \left(\sqrt{ c } \frac{\lambda_x^c \ v\ _2}{2} \right) \frac{v}{\sqrt{ c } \ v\ _2} \right)$	$\exp_x^c(v) = \cosh \left(\sqrt{ c } \ v\ _{\mathcal{L}} \right) x + v \frac{\sinh(\sqrt{ c } \ v\ _{\mathcal{L}})}{\sqrt{ c } \ v\ _{\mathcal{L}}}$
Parallel transport	$PT_{x \rightarrow y}^c(v) = \frac{\lambda_x^c}{\lambda_y^c} \text{gyr}[y, -x]v$	$PT_{x \rightarrow y}^c(v) = v - \frac{c \langle y, v \rangle_{\mathcal{L}}}{1+c \langle x, y \rangle_{\mathcal{L}}} (x + y)$

Geodesics and Induced Distance Function. For a curve $\gamma : [\alpha, \beta] \rightarrow \mathcal{M}$, the shortest length of γ , i.e., geodesics, is defined as $L(\gamma) = \int_{\alpha}^{\beta} \|\gamma'(t)\|_g dt$. Then the distance of $\mathbf{u}, \mathbf{v} \in \mathcal{M}$, $d_{\mathcal{M}}(\mathbf{u}, \mathbf{v}) = \inf L(\gamma)$ where γ is a curve that $\gamma(\alpha) = \mathbf{u}, \gamma(\beta) = \mathbf{v}$.

Maps and Parallel Transport. The maps define the relationship between the hyperbolic space and the corresponding tangent space. For a point $\mathbf{x} \in \mathcal{M}$ and vector $\mathbf{v} \in \mathcal{T}_{\mathbf{x}}\mathcal{M}$, there exists a unique geodesic $\gamma : [0, 1] \rightarrow \mathcal{M}$ where $\gamma(0) = \mathbf{x}, \gamma'(0) = \mathbf{v}$. The exponential map $\exp_{\mathbf{x}} : \mathcal{T}_{\mathbf{x}}\mathcal{M} \rightarrow \mathcal{M}$ is defined as $\exp_{\mathbf{x}}(\mathbf{v}) = \gamma(1)$ and logarithmic map $\log_{\mathbf{x}}$ is the inverse of $\exp_{\mathbf{x}}$. The parallel transport $PT_{\mathbf{x} \rightarrow \mathbf{y}} : \mathcal{T}_{\mathbf{x}}\mathcal{M} \rightarrow \mathcal{T}_{\mathbf{y}}\mathcal{M}$ achieves the transportation from point \mathbf{x} to \mathbf{y} that preserves the metric tensors.

Hyperbolic Models. Hyperbolic geometry is a Riemannian manifold with a constant negative curvature. There exist multiple equivalent hyperbolic models, like the Poincaré ball model, Lorentz model, and Klein model, which show different characteristics but are mathematically equivalent. We here mainly introduce two widely studied and adopted hyperbolic models in HGNNs, i.e., the Poincaré ball model and the Lorentz model. Let $\|\cdot\|$ be the Euclidean norm and $\langle \cdot, \cdot \rangle_{\mathcal{L}}$ denote the Minkowski inner product, respectively. The two models are given by Definition 2.1 and Definition 2.2, respectively. The related formulas and operations, e.g., distances, maps, and parallel transports, are further summarized in Table 1, where \oplus_c and $\text{gyr}[\cdot, \cdot]v$ are Möbius addition [50] and gyration operator [50], respectively.

Definition 2.1 (Poincaré Ball Model). With negative curvature c ($c < 0$), the Poincaré ball model is defined as a Riemannian manifold $(\mathcal{B}_c^n, g_{\mathbf{x}}^{\mathcal{B}})$, where $\mathcal{B}_c^n = \{x \in \mathbb{R}^n : \|x\|^2 < -1/c\}$ is an open n -dimensional ball with radius $1/\sqrt{|c|}$. Its metric tensor $g_{\mathbf{x}}^{\mathcal{B}} = (\lambda_x^c)^2 g^E$, where $\lambda_x^c = 2/(1+c\|x\|_2^2)$ is the conformal factor and g^E is the Euclidean metric, i.e., \mathbf{I}_n .

Definition 2.2 (Lorentz Model). With negative curvature c ($c < 0$), the Lorentz model (also named hyperboloid model) is defined as the Riemannian manifold $(\mathcal{L}_c^n, g_{\mathbf{x}}^{\mathcal{L}})$, where $\mathcal{L}_c^n = \{x \in \mathbb{R}^{n+1} : \langle x, x \rangle_{\mathcal{L}} = 1/c\}$ and $g_{\mathbf{x}}^{\mathcal{L}} = \text{diag}([-1, 1, \dots, 1])_n$.

In the following, we use \mathcal{H} to represent the case that is applicable to both \mathcal{B} and \mathcal{L} . However, in certain situations, we may employ a more precise notation to describe a specific model.

3 HGNN Methodologies

Graph Neural Networks (GNNs) have recently demonstrated significant superiority in graph-related tasks and applications. They excel in explicitly encoding node attributes and their interactions while implicitly capturing high-order dependencies. Hyperbolic GNNs (HGNNs) have further achieved remarkable success in studying graph data, particularly with a tree-like structure, thanks to the unique properties of hyperbolic spaces. Implementing HGNNs involves three fundamental steps: *feature transformation*, *neighborhood aggregation*, and *non-linear activation*. Prior to that, it is necessary to initialize the features by projecting the input Euclidean feature onto the hyperbolic manifold. In the following, we will first introduce the hyperbolic initial layer in Section (3.1) and then present the details of the three steps in Section (3.2), Section (3.3), and Section (3.4), respectively.

3.1 Hyperbolic Initialization Layer

Consider a graph $\mathcal{G} = (\mathcal{V}, \mathcal{E})$ with a vertex set \mathcal{V} and an edge set \mathcal{E} . Let $(\mathbf{x}_i^E)_{i \in \mathcal{V}}$ represent the n -dimensional input node features, where $\mathbf{x}_i^E \in \mathbb{R}^n$ and the superscript E indicates the Euclidean space. For each vertex $i \in \mathcal{V}$, its n -dimensional input node feature is denoted as \mathbf{x}_i^H , residing in the Euclidean space. To refer to the tangent state at \mathbf{x} and the hyperbolic state (in either the Poincaré ball model or the Lorentz model), we will use the superscripts

$\mathcal{T}_\mathbf{x}$ and $\mathcal{H}(\mathcal{B}/\mathcal{L})$, respectively. In the existing literature, the Euclidean node features \mathbf{x}^E is typically derived from four different sources: (i) pre-trained embedding [48, 7], (ii) directly from node attributes [5, 29, 73], (iii) randomly sampling [33, 34, 42, 65, 64, 43] or (iv) one-hot projection [38, 66, 63].

Initialization layer in Poincaré ball model. To project the feature \mathbf{x}^E onto the Poincaré ball model \mathcal{B} , the exponential map is commonly used. This can be expressed as:

$$\mathbf{x}^{\mathcal{B}} = \exp_{\mathbf{o}}^c(\mathbf{x}^E), \quad (1)$$

where the \mathbf{x}^E is interpreted as a node situated in the tangent space at the origin, that is $\mathbf{x}^E \in \mathcal{T}_{\mathbf{o}}\mathcal{B}^n$.

Initialization layer in Lorentz model. In the Lorentz model, a similar approach is adopted. Notably, when considering \mathbf{x}^E as a point in the tangent space at the origin, it becomes necessary to prepend a zero value to \mathbf{x}^E [5]. Thus, we have $\mathbf{x}^{\mathcal{T}_\mathbf{o}} = (0, \mathbf{x}^E)$, satisfying the condition $\langle 0, (0, \mathbf{x}^E) \rangle_{\mathcal{L}} = 0$. This point is then projected into the Lorentz model using the exponential map:

$$\mathbf{x}^{\mathcal{L}} = \exp_{\mathbf{o}}^c(\mathbf{x}^{\mathcal{T}_\mathbf{o}}) = \exp_{\mathbf{o}}^c((0, \mathbf{x}^E)). \quad (2)$$

Besides, Gulcehre et al. introduced a projection using pseudo polar coordinates, which has the same final expression as the Equation (2).

Once we have obtained the initialization state of the nodes, we proceed with feature transformation and neighborhood aggregation, followed by non-linear activation. The current methods primarily utilize two approaches for these transformations: the tangent space approach and the fully hyperbolic transformation.

- In the tangent space method, nodes are initially mapped to the tangent space using the logarithmic map. As the tangent space is isomorphic to the Euclidean space, the transformation takes place there. Subsequently, the nodes are mapped back to the hyperbolic space using the exponential map.
- The fully hyperbolic transformation is conducted entirely within the hyperbolic space without any involvement of the tangent space.

3.2 Hyperbolic Feature Transformation

Hyperbolic feature transformation mainly consists of matrix-vector multiplication and bias addition. In the subsequent sections, we will provide a detailed review of these operations.

Matrix-vector Multiplication. To implement matrix-vector multiplication, the tangential method is applicable for both the Poincaré ball model and the Lorentz model. Let $\mathbf{x}^{\mathcal{B}} \in \mathcal{B}_c^n$, $\mathbf{W} \in \mathbb{R}^{d \times n}$, then in Poincaré ball model, the matrix-vector multiplication [14, 29] is defined by

$$\mathbf{W} \otimes_c^{\mathcal{B}} \mathbf{x}^{\mathcal{B}} := \exp_{\mathbf{o}}^c(\mathbf{W} \log_{\mathbf{o}}^c(\mathbf{x}^{\mathcal{B}})). \quad (3)$$

The node features $\mathbf{x}^{\mathcal{B}}$ are projected from the Poincaré ball model to the tangent space, which is isometric to Euclidean space. After performing the matrix-vector multiplication operation in the tangent space, they are mapped back to the Poincaré ball.

In the context of the Lorentz model, one method to achieve matrix-vector multiplication is similar to that of the Poincaré ball model. Chami et al. directly employed Equation (3) on the Lorentz model. However, this approach breaks the constraints inherent to the Lorentz manifold. To rectify this, it is imperative that the node features remain within the tangent space at the origin after the matrix \mathbf{M} multiplication³. As suggested by [75, 66], this can be accomplished by modifying the values of the last n coordinates. The formula is defined by

$$\mathbf{W} \otimes_c^{\mathcal{L}} \mathbf{x}^{\mathcal{L}} := \exp_{\mathbf{o}}^c(0, \mathbf{W} \log_{\mathbf{o}}^c(\mathbf{x}^{\mathcal{L}})_{[1:n]}), \quad (4)$$

where $\mathbf{x}^{\mathcal{L}} \in \mathcal{L}_c^n$, $\mathbf{W} \in \mathbb{R}^{d \times n}$. This method ensures the first coordinate is consistently zero, signifying that the resultant transformation is invariably within the tangent space at \mathbf{o} .

Furthermore, Dai et al. defined a new matrix for the Lorentz feature transformation as:

$$\begin{aligned} \mathbf{W} \otimes \mathbf{x}^{\mathcal{L}} &:= \mathbf{W} \mathbf{x}^{\mathcal{L}} \\ \text{s.t. } \mathbf{W} &= \begin{bmatrix} 1 & \mathbf{0}^\top \\ \mathbf{0} & \widehat{\mathbf{M}} \end{bmatrix}, \widehat{\mathbf{M}}^\top \widehat{\mathbf{M}} = \mathbf{I}, \end{aligned} \quad (5)$$

³Supposing we use Lorentz origin as the reference point.

Table 2: Summary of neighborhood aggregation weight in HGNNs. SI: structure information; FI: feature information; HD: hyperbolic distance.

Formula	Source	Reference	Description
$\alpha_{ij} = 1/\sqrt{\tilde{d}_i \tilde{d}_j}$	SI	[29]	Simplified spectral convolution based on node degree d_i, d_j
$\alpha_{ij} = \text{softmax}_{j \in N(i)}(\text{MLP}(\kappa_{i,j}))$	SI	[67]	Curvature-based weight κ sensitive to local graph structure
$\alpha_{ij} = \text{softmax}_{j \in N(i)}(\text{LeakReLU}(\mathbf{W}^T[\mathbf{x}_i^{\mathcal{T}_0}; \mathbf{x}_j^{\mathcal{T}_0}]))$	FI	[5]	Weighting adaptive to node feature \mathbf{x}
$\alpha_{ij} = \text{softmax}_{j \in N(i)}(-d_c(\mathbf{x}_i^{\mathcal{H}}, \mathbf{x}_j^{\mathcal{H}}))$	HD	[74]	Based on negative hyperbolic distance d_c between nodes
$\alpha_{ij} = \text{softmax}_{j \in N(i)}(-d_c^2(\mathbf{x}_i^{\mathcal{H}}, \mathbf{x}_j^{\mathcal{H}}))$	HD	[75, 8]	Weighting with squared hyperbolic distance, emphasizing geometry
$\alpha_{ij} = f(-\beta d_c(\mathbf{x}_i^{\mathcal{H}}, \mathbf{x}_j^{\mathcal{H}}) - \gamma)$	HD	[17]	Flexible weighting incorporating squared hyperbolic distance d_c^2
$\alpha_{ij} = \text{softmax}_{j \in N(i)}(\text{LeakReLU}(\mathbf{W}^T[\mathbf{x}_i; \mathbf{x}_j]) \times d_c(\mathbf{x}_i^{\mathcal{H}}, \mathbf{x}_j^{\mathcal{H}}))$	FI,HD	[77]	Combines hyperbolic distance d_c with node feature \mathbf{x}
$\alpha_{ij} = \text{sigmoid}(\text{LeakReLU}(\mathbf{W}^T[\mathbf{x}_i; \mathbf{x}_j]) \times \frac{1}{\sqrt{d_i d_j}})$	FI,SI	[5]	Integrates node feature \mathbf{x} with node degree information d_i, d_j
$\alpha_{ij} = \frac{w_{\kappa} \kappa_{ij} + w_f \tilde{f}_{ij}}{w_{\kappa} + w_f}$	FI,SI	[67]	Unifies node curvature information w_{κ} with node feature w_f

where $\mathbf{W} \in \mathbb{R}^{n+1}$, $\widehat{\mathbf{M}}$ is a transformation sub-matrix, acting as a rotation matrix. $\mathbf{0}$ is a column vector of zeros, and \mathbf{I} is an identity matrix. Compared to Equation (4), this method employs $\widehat{\mathbf{M}}$ to define \mathbf{W} . This transformation respects the Lorentz constraints, let \mathbf{y} be the result, then we have the following:

$$\begin{aligned}
 \langle \mathbf{y}, \mathbf{y} \rangle_{\mathcal{L}} &= -x_0^2 + (\widehat{\mathbf{M}} \mathbf{x}_{1:n})^{\top} \widehat{\mathbf{M}} \mathbf{x}_{1:n} \\
 &= -x_0^2 + \mathbf{x}_{1:n}^{\top} (\widehat{\mathbf{M}}^{\top} \widehat{\mathbf{M}}) \mathbf{x}_{1:n} \\
 &= -x_0^2 + \mathbf{x}_{1:n}^{\top} \mathbf{x}_{1:n} \\
 &= -1.
 \end{aligned} \tag{6}$$

Then, it is derived that the transformed result \mathbf{y} lies in the Lorentz model. Recent study [8] shows that the above linear transformation only considers a special rotation but no boost. They then derived a general transformation method, which is equipped with both rotation and boost operations as well bias addition, normalization, etc., i.e.,

$$\mathbf{W} \otimes_c^{\mathcal{L}} \mathbf{x}^{\mathcal{L}} = \left(\begin{bmatrix} \mathbf{v}^{\top} \\ \mathbf{M} \end{bmatrix} \right) \otimes_c^{\mathcal{L}} \mathbf{x}^{\mathcal{L}} = \begin{bmatrix} \sqrt{\|\phi(\mathbf{M}\mathbf{x}, \mathbf{v})\|^2 - 1/K} \\ \phi(\mathbf{M}\mathbf{x}, \mathbf{v}) \end{bmatrix}, \tag{7}$$

where $\phi(\mathbf{M}\mathbf{x}, \mathbf{v}) = \frac{\lambda \sigma(\mathbf{v}^{\top} \mathbf{x} + b')}{\|\mathbf{M}h(\mathbf{x}) + \mathbf{b}\|} (\mathbf{M}h(\mathbf{x}) + \mathbf{b})$, where σ is the sigmoid function, \mathbf{b} and b' are bias terms, $\lambda > 0$ controls the scaling range, h is the activation function.

In general, implementing feature transformation in HGNN is mainly composed of two different methods: tangent space method, fully in the hyperbolic manifold.

Bias Addition. To implement bias addition, tangent space at origin is still a useful medium, and the formula in \mathcal{B} and \mathcal{L} can be uniformly expressed as:

$$\mathbf{x}^{\mathcal{H}} \oplus_c^{\mathcal{H}} \mathbf{b}^{\mathcal{H}} = \exp_{\mathbf{x}^{\mathcal{H}}}^c(P_{\mathbf{o} \rightarrow \mathbf{x}^{\mathcal{H}}}^c(\log_{\mathbf{o}}^c(\mathbf{b}^{\mathcal{H}}))), \tag{8}$$

where $\mathbf{b}^{\mathcal{H}}$ is the bias in \mathcal{H}_c^n , and the equations of parallel transport $P_{\mathbf{x}^{\mathcal{H}} \rightarrow \mathbf{y}^{\mathcal{H}}}^c(\cdot)$ in \mathcal{B} and \mathcal{L} are summarized in Table 1. In [8], they incorporated the bias addition in Equation (7).

3.3 Hyperbolic Neighborhood Aggregation

Hyperbolic neighborhood aggregation is a technique that leverages the hyperbolic space to aggregate information from neighboring nodes in a graph. This process can be broadly divided into two main steps: (1) computation of neighborhood weights and (2) computation of mean aggregation.

Computation of neighborhood weights. The determination of neighborhood weights is crucial in aggregating information effectively. Various strategies can be employed to calculate these weights, including utilizing structure information, feature information, hyperbolic distance, or a combination of these methods, which are summarized in Table 2. Below, we delve into each of these strategies. Consider a central node i , and we assume that $N(i)$ represents the immediate one-hop neighbor of node i , with j being an element of $N(i)$ ⁴.

(1) *Structure information:* The weight α_{ij} can be defined based on node degree [29]:

$$\alpha_{ij} = 1/\sqrt{\tilde{d}_i \tilde{d}_j}, \tag{9}$$

⁴Following the literature, we consider $i \in N(i)$.

where $\tilde{d}_i = d_i + 1$ and d_i is the degree of node i . This method, derived from the Euclidean graph convolutional network [23], provides a simplified approach to graph spectral convolution, primarily focusing on the topological information of the graph.

Additionally, the weight can also be defined using Ollivier Ricci curvature [35], which describes the deviation of a local pair of neighborhoods from a "flat" case,

$$\alpha_{ij} = \text{softmax}_{j \in N(i)} (\text{MLP}(\kappa_{i,j})), \quad (10)$$

where MLP represents Multi-layer Perception and curvature κ reflects the local structure of the node i , which is computed by optimal transport [67].

(2) *Feature information* [5]: The weight α_{ij} using node feature is defined as follows:

$$\alpha_{ij} = \text{softmax}_{j \in N(i)} (\text{LeakReLU}(\mathbf{W}^T[\mathbf{x}_i^{\mathcal{T}_0} || \mathbf{x}_j^{\mathcal{T}_0}])). \quad (11)$$

This method computes the weight based on the hyperbolic features of nodes i and j , drawing inspiration from the graph attention network [53].

(3) *Hyperbolic distance* [74]: The weight α_{ij} is formulated as:

$$\alpha_{ij} = \text{softmax}_{j \in N(i)} (-d_{\mathcal{H}}^c(\mathbf{x}_i^{\mathcal{H}}, \mathbf{x}_j^{\mathcal{H}})). \quad (12)$$

This equation computes the weight based on the hyperbolic distance between nodes i and j . The negative sign ensures that closer nodes have higher weights. Besides, Zhang et al. also introduced K -head attention, which is defined as:

$$\alpha_{ij} = \text{softmax}_{j \in N(i)} \left(-\sqrt{\sum_{k=1}^K d_{\mathcal{H}}^c(\mathbf{x}_i^{\mathcal{H},k}, \mathbf{x}_j^{\mathcal{H},k})} \right).$$

Alternative approaches using hyperbolic distance include using squared distance [75]:

$$\alpha_{ij} = \text{softmax}_{j \in N(i)} (-d_{\mathcal{H}}^c(\mathbf{x}_i^{\mathcal{H}}, \mathbf{x}_j^{\mathcal{H}})^2). \quad (13)$$

Similar to the previous method, the distance is squared, emphasizing the difference between close and distant nodes. Another more complex form [17] is given as:

$$\alpha_{ij} = f(-\beta d_{\mathcal{H}}^c(\mathbf{x}_i^{\mathcal{H}}, \mathbf{x}_j^{\mathcal{H}}) - \gamma), \quad (14)$$

where β and γ are parameters that can be set manually or learned along with the training process, and f can be $\text{softmax}(\cdot)$. The hyperbolic distance is scaled by a factor β and shifted by γ . Both β and γ can be learned or set manually. The function f can be a softmax function, ensuring the weights are normalized.

(4) *Integration of feature information and hyperbolic distance* [76]: The α_{ij} is computed by

$$\alpha_{ij} = \text{softmax} \left(\text{LeakReLU}(\mathbf{W}^T[\mathbf{x}_i^{\mathcal{T}_0} || \mathbf{x}_j^{\mathcal{T}_0}]) \times d_{\mathcal{H}}^c(\mathbf{x}_i^{\mathcal{H}}, \mathbf{x}_j^{\mathcal{H}}) \right). \quad (15)$$

This approach combines feature attention and node distance. Compared with the pure feature method, it is modulated by the hyperbolic distance between the nodes, ensuring that both the node features and their relative positions in the hyperbolic space contribute to the weight.

(5) *Integration of feature and structure information*: The weight α_{ij} is computed by⁵

$$\alpha_{ij} = \text{sigmoid} \left(\text{LeakReLU}(\mathbf{W}^T[\mathbf{x}_i^{\mathcal{T}_0} || \mathbf{x}_j^{\mathcal{T}_0}]) \right) \times 1/\sqrt{\tilde{d}_i \tilde{d}_j}. \quad (16)$$

This method integrates both structural information and feature attention, ensuring that both the node features and their connectivity in the graph contribute to the weight. In [67], Yang et al. introduced another integration, which is formulated by:

$$\alpha_{ij} = \frac{w_{\kappa} \tilde{\kappa}_{ij} + w_f \tilde{f}_{ij}}{w_{\kappa} + w_f},$$

where $\tilde{\kappa}_{ij}$ and \tilde{f}_{ij} is derived from Equation (10) and (11), respectively.

Computation of Mean Aggregation. For mean aggregation, or weighted mean pooling, it cannot be computed by simply averaging the inputs, which may lead a deviation out of the hyperbolic manifold. Currently, there are three

⁵From <https://github.com/HazyResearch/hgcn>

typical ways to implement mean aggregation: tangential method, Einstein midpoint, and Lorentzian centroid.

(1) Tangential method [29, 5] is defined by,

$$\text{AGG}(\mathbf{x}_i^{\mathcal{H}}) := \exp_{\mathbf{o}}^c \left(\sum_{j \in \mathcal{N}_i} \alpha_{ij} (\log_{\mathbf{o}}^c(\mathbf{x}_i^{\mathcal{H}})) \right). \quad (17)$$

(2) Einstein midpoint method [17, 10] is formulated as,

$$\text{AGG}(\mathbf{x}_i^{\mathcal{H}}) := \begin{cases} \bar{\mathbf{x}}_j^{\mathcal{K}} = p_{\mathcal{H} \rightarrow \mathcal{K}}(\mathbf{x}_j^{\mathcal{H}}) \\ \mathbf{m}_i^{\mathcal{K}} = \sum_{j \in \mathcal{N}_i} \gamma_j \bar{\mathbf{x}}_j^{\mathcal{K}} / \sum_{j \in \mathcal{N}_i} \gamma_j, \\ \mathbf{x}_i^{\mathcal{H}} = p_{\mathcal{K} \rightarrow \mathcal{H}}(\mathbf{m}_i^{\mathcal{K}}) \end{cases} \quad (18)$$

where $p_{\mathcal{M}_1 \rightarrow \mathcal{M}_2}$ denotes the projection from \mathcal{M}_1 to \mathcal{M}_2 and $\gamma_j = (1 - \|\bar{\mathbf{x}}_j^{\mathcal{K}}\|^2)^{-1/2}$ is the Lorentz factor.

(3) Lorentzian centroid method [75, 8, 38] is expressed as,

$$\text{AGG}(\mathbf{x}_i^{\mathcal{L}}) := \frac{\sum_{j \in \mathcal{N}_i} \alpha_{ij} \mathbf{x}_j^{\mathcal{L}}}{\sqrt{c} \|\sum_{j \in \mathcal{N}_i} \alpha_{ij} \mathbf{x}_j^{\mathcal{L}}\|_{\mathcal{L}}}. \quad (19)$$

The tangential mean computation is one of the most straightforward methods. It is applicable to the Poincaré ball and Lorentz models. However, directly executing the weighted mean in the tangent space needs extra caution to guarantee the results still live in the manifold. On the other hand, it lacks a differentiable Fréchet mean operation [30]. The Einstein midpoint is based on the Klein coordinates and applicable to Poincaré ball and Lorentz models by the isomorphic bijections. The Lorentzian centroid is designed for Lorentz model. Besides, there is another equivalent centroid for Poincaré ball model as shown in [41], i.e., Möbius gyromidpoint [51]. These three centroids can be characterized as a minimizer of the weighted sum of calibrated squared distance [41].

3.4 Non-linear Activation

The non-linear activation can be achieved with the same idea of matrix-vector multiplication [5], i.e.,

$$\sigma^{\otimes^{c_{\ell-1}, c_{\ell}}}(\mathbf{x}^{\mathcal{H}}) = \exp_{\mathbf{o}}^{c_{\ell}}(\sigma(\log_{\mathbf{o}}^{c_{\ell-1}}(\mathbf{x}^{\mathcal{H}}))), \quad (20)$$

where ℓ denotes the $\ell - th$ layer. For the Lorentz model, [75] proposed a more accurate form,

$$\sigma^{\otimes^{c_{\ell-1}, c_{\ell}}}(\mathbf{x}^{\mathcal{H}}) = \exp_{\mathbf{o}}^{c_{\ell}}(0, \sigma(\log_{\mathbf{o}}^{c_{\ell-1}}(\mathbf{x}_{[1:n]}^{\mathcal{H}}))), \quad (21)$$

which ensures that the result still lives in the Lorentz manifold. Besides, according to the manifold-preserving properties between the Lorentz model and Poincaré ball model, another way is to convert the Lorentzian feature to the Poincaré feature and implement the non-linearity in Poincaré ball model [10]

$$\sigma^{\otimes^{c_{\ell-1}, c_{\ell}}}(\mathbf{x}^{\mathcal{H}}) = p_{\mathcal{B} \rightarrow \mathcal{H}}(\sigma(p_{\mathcal{H} \rightarrow \mathcal{B}}(\mathbf{x}^{\mathcal{H}})))$$

Chen et al. incorporated the non-linear activation in Equation (7). Since the exponential map is a non-linear operation, which can produce the non-linearity, works by [42, 55] thus ignored it.

3.5 Overall View

In general, a unified hyperbolic graph convolutional layer can be formulated as,

$$\begin{aligned} \mathbf{h}_i^{\ell, \mathcal{H}} &= \left(\mathbf{W}^{\ell} \otimes^{c_{\ell-1}} \mathbf{x}_i^{\ell-1, \mathcal{H}} \right) \oplus^{c_{\ell-1}} \mathbf{b}^{\ell}, \\ \mathbf{y}_i^{\ell, \mathcal{H}} &= \text{AGG}^{c_{\ell-1}}(\mathbf{h}_i^{\ell, \mathcal{H}})_i, \\ \mathbf{x}_i^{\ell, \mathcal{H}} &= \sigma^{\otimes^{c_{\ell-1}, c_{\ell}}}(\mathbf{y}_i^{\ell, \mathcal{H}}). \end{aligned} \quad (22)$$

To reduce the maps between tangent space and hyperbolic manifold, some research works, for example, [29], achieve all three steps in the tangent space. Although this simplification can reduce some computation burden, its performance decreases as well, according to the experimental results [76].

4 Applications

Hyperbolic spaces have many successful applications in a variety of fields, including natural language processes, computer vision, etc., while the applications of HGNNS are mainly on recommendation systems, knowledge graphs, and drug molecules, where the dataset is graph-structured in natural and have the tree-like characteristic.

4.1 HGNNs for Recommender Systems

The recommender systems can be simplified as a bipartite graph, in which vertices represent users or items, and edges denote their interactions. Considering the prevalence of the power-law distribution in user-item networks, hyperbolic space has attracted considerable attention. In the following, we review the recommender systems built upon hyperbolic space from four aspects.

Graph Neural Collaborative Filtering. In the settings of graph neural collaborative filtering, the features of items and users are often not available. [42, 55, 65] built the feature via Gaussian sampling. Further, they incorporate multiple layers of HGNN to gather higher-order information for explicitly modeling user-item interactions.

Social Network Enhanced Recommender System. Apart from user-item interactions, users' preferences are strongly tied to their social relationships (e.g., friends and followers). [54] designed a multi-aspect perceiving HGNN in hyperbolic space to capture multi-aspect interactions of users on item, via defining a learnable interactive relation for each specific user-item pair.

Knowledge Graph Enhanced Recommender System. Recommender systems incorporating the knowledge graph as side information can not only address the issues of data sparsity and cold start issues but also provide explanations for recommended items. [9] proposed a Lorentzian knowledge-enhanced graph convolutional network for recommendation, which extracts high-order interaction in user-item bipartite graphs and knowledge graph for recommendation.

Session-based Recommender System. Session-based recommendation learns the user preferences by analyzing the short-term and long-term patterns based on the user behavior. [18] proposed a contrastive learning manner for session-based recommendation and [27] presented a hyperbolic space-based hypergraph convolutional neural network to learn for session-based recommender systems.

4.2 HGNNs for Knowledge Graph

The knowledge graph is a graph-structured network representing real-world facts with triplets to store a large number of entity and relation information. Given that in large-scale knowledge graphs, the number of entities is scale-free and can be organized to the underlying hierarchical structure, hyperbolic geometry thus provides a powerful alternative to learning low-dimensional embedding while preserving the underlying hierarchy.

Knowledge graph completion and associations are two important applications. [57] proposed an attentive neural context aggregation to adaptively integrate the relational context for enhancing the ability to preserve the hierarchical relations. Moreover, [58] explored the mixed curvature for knowledge graph completion. For HGNN-based knowledge graph associations, [45] developed a HyperKA model that employs an HGNN for KG embedding and utilizes a hyperbolic transformation across embedding spaces to capture multi-granular knowledge associations.

Compared with the hyperbolic transnational model for knowledge graph, e.g., KypKG [24] MuRP [1], AttH [6], and HERCULES [31], HGNN-based models show more competitive performance with further extracting and incorporating high-order relationships.

4.3 HGNNs for Molecular

Molecules are also naturally represented as graphs, with nodes representing atoms and edges representing chemical bonds. Recently, many studies used GNNs and some of their variations to predict chemical properties. For molecular applications, the research mainly focuses on molecular representation and generation. The basic motivation to apply hyperbolic spaces on molecules is to model the underlying hierarchical structure in it.

Molecular Representation. [60] developed a hyperbolic relational graph convolution network plus (HRGCN+) by combining molecular graphs and molecular descriptors for drug discovery. HRGCN+ allows medicinal chemists to understand models at both the atom and descriptor levels, which can also aid in the extraction of hidden information. [68] proposed to learn molecular embedding through the hyperbolic VAE framework to discover new side effects and re-position drugs.

Molecular Generation. Learning the implicit structure of molecules using hyperbolic space is an important method for extracting molecular latent hierarchical structure. Hyperbolic molecule generation is generally via graph generation models, including normalized flow [2], GAN [38], etc.

4.4 HGNNs for Other Applications

In this part, we will discuss more successful applications of HGNNs from different fields. For skeleton-based action recognition, [36] designed a hyperbolic spatial-temporal GCN that combines several dimensions on the manifold and provides an effective technique to explore the dimension for each ST-GCN layer. For quantitative trading and investment decision making, [40] modeled the inter-stock relations by HGNN and developed a stock model HyperStockGAT, which constructs the stock graph by the relation in Wikidata and their industry information. For medical ontology matching, [20] proposed MEDTO framework, which is built upon HGNN and a heterogeneous graph layer.

5 Challenges and Opportunities

Although we have witnessed the rapid development and achievements of HGNNs in recent years, there are still issues and challenges that need better solutions. [37] discussed several open problems which are also shared by HGNNs. In this section, we further summarize several challenges in the HGNN community, which also provides opportunities for future study.

5.1 Challenges I: Complex Structures

In graph representation learning, hyperbolic space is emerging as a potential alternative. The most noticeable advantages are credited to its exponential volume growth property, which makes this space to be much more embeddable than Euclidean space, especially for datasets with implicit tree-like layouts. However, the structure of a real-world network is always complex and complicated, in which some areas are tree-like, some are flat and some are circular. Directly embedding a graph with intricate layouts into the hyperbolic manifold inevitably leads to structural inductive biases and distortions.

Opportunities: To this point, there are some preliminary attempts, but there is still much potential for improvements. An intuitive approach is to combine Euclidean and/or spherical spaces to complement the hyperbolic space. For example, GIL [76] utilizes hyperbolic space and Euclidean space interactively and places different weights on two branches to cope with intricate complex graph structures. M²GNN [58] incorporates three different spaces, namely hyperbolic, Euclidean, and spherical spaces, for knowledge graph completion. SelfMGNN [44] resorts to a mixed-curvature space via the Cartesian product. On the other hand, ACE-HGNN [13] attempts to learn an optimal curvature to model the tree-like graph with different hyperbolicity via a multi-agent reinforcement learning framework. HGCL [28] enhances the modeling of HGNN by contrastive learning. These methods generally need to create multiple branches, which unavoidably increases the computational complexity to a certain extent. Besides, most of the above methods solve this issue in a global manner. A local identifier, like Ricci curvature [32, 49] can be more effective and efficient.

5.2 Challenge II: Geometry-aware Learning

Though HGNNs have made noticeable achievements, most of the efforts mainly focus on how to generalize GNNs into hyperbolic space by properly designing the transformation operations among the spaces. In many HGNNs, the optimization target (like cross-entropy in [5] and [75]) are generally similar to the Euclidean counterparts, which are geometrically irreverent with hyperbolic properties. On the other hand, hyperbolic space is curved, that is, locations closer to the origin are flatter and relatively narrow, whereas regions further from the origin are broader, and this property is seldom considered when designing HGNNs.

Opportunities: From the optimization target, how to integrate the hyperbolic geometry with the learning objective is the *first* valuable problem to explore. Recently, [65] presented a geometrically aware hyperbolic recommender system, paving the path for the community. The *second* opportunity is to make the learning process geometry-aware, keeping the awareness of node position rather than being equipped with a geometry-unconscious optimization target, like the constant margin in metric learning. *Last*, based on the hyperbolic geometric trait, the exponentially hyperbolic space provides spacious room for the samples to be well arranged, especially in the area far away from the origin. Intuitively, by encouraging the model to preserve the inherent data structure and pushing the overall embedding far away from the origin, the model representation ability could then be largely improved.

5.3 Challenges III: Trustworthy HGNNs

HGNNs have been proven to produce better representations of hierarchical graphs. However, there are still a few trustworthy issues to be addressed: (1) Where is the superiority of the hyperbolic space? For example, the better performance of the hyperbolic model originates from where? the better fitting of high-level nodes, tail nodes, or both?

(2) It is unclear in what conditions the HGNNs are guaranteed to be better than their Euclidean counterparts. In other words, the generalization error and the robustness of HGNNs have not been well studied and analyzed.

Opportunities: [72] made an initial study empirically investigating the behavior of hyperbolic recommender systems. To figure out the characteristics of HGNNs, more in-depth analyses are needed. For the generalization ability, [46] pointed out that in hyperbolic ordinal embedding (HOE), the generalization error bound is at most exponential with respect to the embedding radius and HOE can represent a tree better than linear graph embedding [47]. The analysis facilitates the exploration of the generalization and robustness of HGNNs.

5.4 Challenges IV: Scalable HGNNs

Despite the tremendous success in the performance improvement, HGNNs also bring in more computational requirements compared with their Euclidean counterparts, e.g., the frequent exponential and logarithmic maps [69]. In real-world scenarios, graphs often on the scale of millions of nodes and edges, and computational resources are limited. The difficulty of extending HGNNs to large-scale graphs remains one of the main challenges.

Opportunities: A large body of research work has been proposed to improve the scalability of GNNs by decoupling the graph process, simplifying the feature transformation or aggregation operations [59, 12], or via a series sampling techniques [70, 19, 21], which could be further integrated with the property of HGNNs.

6 Conclusion

Hyperbolic space can be regarded as a continuous tree, making it well-suited for modeling datasets with latent hierarchy layouts. HGNNs extend GNNs into hyperbolic space and have achieved great success in graph data, especially with tree-like structures. In this survey, we present the technical details of HGNNs, including the methodologies, applications, challenges, opportunities, and current state-of-the-art models and algorithms of HGNN networks. More specifically, we unify them by a general framework and summarize the variants of each module. We also identified several challenges that need to be overcome. To some extent, these challenges serve as guidelines for flourishing the achievements of hyperbolic graph learning. Although many researchers are actively engaged in addressing these problems, we point to the numerous opportunities that still exist to contribute to the development of this important, ever-evolving field.

References

- [1] Ivana Balazevic, Carl Allen, and Timothy M. Hospedales. Multi-relational poincaré graph embeddings. In *NeurIPS*, pages 4465–4475, 2019.
- [2] Avishek Joey Bose, Ariella Smofsky, Renjie Liao, Prakash Panangaden, and William L Hamilton. Latent variable modelling with hyperbolic normalizing flows. In *ICML*, pages 1045–1055, 2020.
- [3] Guillaume Bouchard, Sameer Singh, and Theo Trouillon. On approximate reasoning capabilities of low-rank vector spaces. In *AAAI spring symposia*, 2015.
- [4] Michael M Bronstein, Joan Bruna, Yann LeCun, Arthur Szlam, and Pierre Vandergheynst. Geometric deep learning: going beyond euclidean data. *IEEE Signal Processing Magazine*, 34(4):18–42, 2017.
- [5] Ines Chami, Zhitao Ying, Christopher Ré, and Jure Leskovec. Hyperbolic graph convolutional neural networks. In *NeurIPS*, pages 4868–4879, 2019.
- [6] Ines Chami, Adva Wolf, Da-Cheng Juan, Frederic Sala, Sujith Ravi, and Christopher Ré. Low-dimensional hyperbolic knowledge graph embeddings. In *ACL*, pages 6901–6914. ACL, 2020.
- [7] Boli Chen, Yao Fu, Guangwei Xu, Pengjun Xie, Chuanqi Tan, Mosha Chen, and Liping Jing. Probing bert in hyperbolic spaces. *arXiv preprint arXiv:2104.03869*, 2021.
- [8] Weize Chen, Xu Han, Yankai Lin, Hexu Zhao, Zhiyuan Liu, Peng Li, Maosong Sun, and Jie Zhou. Fully hyperbolic neural networks. *arXiv preprint arXiv:2105.14686*, 2021.
- [9] Yankai Chen, Menglin Yang, Yingxue Zhang, Mengchen Zhao, Ziqiao Meng, Jianye Hao, and Irwin King. Modeling scale-free graphs for knowledge-aware recommendation. *WSDM*, 2022.
- [10] Jindou Dai, Yuwei Wu, Zhi Gao, and Yunde Jia. A hyperbolic-to-hyperbolic graph convolutional network. In *CVPR*, pages 154–163, 2021.
- [11] Federico Errica, Marco Podda, Davide Bacciu, and Alessio Micheli. A fair comparison of graph neural networks for graph classification. In *ICLR*, 2019.

[12] Fabrizio Frasca, Emanuele Rossi, Davide Eynard, Benjamin Chamberlain, Michael Bronstein, and Federico Monti. SIGN: Scalable inception graph neural networks. In *ICML GRL workshop*, 2020.

[13] Xingcheng Fu, Jianxin Li, Jia Wu, Qingyun Sun, Cheng Ji, Senzhang Wang, Jiajun Tan, Hao Peng, and S Yu Philip. ACE-HGNN: Adaptive curvature exploration hyperbolic graph neural network. In *ICDM*, pages 111–120, 2021.

[14] Octavian Ganea, Gary Bécigneul, and Thomas Hofmann. Hyperbolic neural networks. In *NeurIPS*, pages 5345–5355, 2018.

[15] Aditya Grover and Jure Leskovec. node2vec: Scalable feature learning for networks. In *KDD*, pages 855–864, 2016.

[16] Caglar Gulcehre, Misha Denil, Mateusz Malinowski, Ali Razavi, Razvan Pascanu, Karl Moritz Hermann, Peter Battaglia, Victor Bapst, David Raposo, Adam Santoro, et al. Hyperbolic attention networks. *ICLR*, 2019.

[17] Caglar Gulcehre, Misha Denil, Mateusz Malinowski, Ali Razavi, Razvan Pascanu, Karl Moritz Hermann, Peter Battaglia, Victor Bapst, David Raposo, Adam Santoro, et al. Hyperbolic attention networks. In *ICLR*, 2019.

[18] Naicheng Guo, Xiaolei Liu, Shaoshuai Li, Qiongxu Ma, Yunan Zhao, Bing Han, Lin Zheng, Kaixin Gao, and Xiaobo Guo. HCGR: Hyperbolic contrastive graph representation learning for session-based recommendation. *arXiv preprint arXiv:2107.05366*, 2021.

[19] William L Hamilton, Rex Ying, and Jure Leskovec. Inductive representation learning on large graphs. In *NeurIPS*, pages 1025–1035, 2017.

[20] Junheng Hao, Chuan Lei, Vasilis Efthymiou, Abdul Quamar, Fatma Özcan, Yizhou Sun, and Wei Wang. Medto: Medical data to ontology matching using hybrid graph neural networks. In *KDD*, pages 2946–2954, 2021.

[21] Zengfeng Huang, Shengzhong Zhang, Chong Xi, Tang Liu, and Min Zhou. Scaling up graph neural networks via graph coarsening. In *KDD*, pages 675–684, 2021.

[22] Thomas N Kipf and Max Welling. Variational graph auto-encoders. *Bayesian Deep Learning Workshop (NIPS 2016)*, 2016.

[23] Thomas N Kipf and Max Welling. Semi-supervised classification with graph convolutional networks. In *ICLR*, 2017.

[24] Prodromos Kolivakis, Alexandros Kalousis, and Dimitris Kiritsis. HyperKG: Hyperbolic knowledge graph embeddings for knowledge base completion. *arXiv preprint arXiv:1908.04895*, 2019.

[25] John M Lee. *Riemannian manifolds: an introduction to curvature*, volume 176. Springer Science & Business Media, 2006.

[26] John M Lee. Smooth manifolds. In *Introduction to Smooth Manifolds*, pages 1–31. Springer, 2013.

[27] Yicong Li, Hongxu Chen, Xiangguo Sun, Zhenchao Sun, Lin Li, Lizhen Cui, Philip S Yu, and Guandong Xu. Hyperbolic hypergraphs for sequential recommendation. In *CIKM*, 2022.

[28] Jiahong Liu, Menglin Yang, Min Zhou, Shanshan Feng, and Philippe Fournier-Viger. Enhancing hyperbolic graph embeddings via contrastive learning. In *NeurIPS 2nd SSL workshop*, 2022.

[29] Qi Liu, Maximilian Nickel, and Douwe Kiela. Hyperbolic graph neural networks. In *NeurIPS*, pages 8230–8241, 2019.

[30] Aaron Lou, Isay Katsman, Qingxuan Jiang, Serge Belongie, Ser-Nam Lim, and Christopher De Sa. Differentiating through the fréchet mean. In *ICML*, pages 6393–6403. PMLR, 2020.

[31] Sébastien Montella, Lina Maria Rojas-Barahona, and Johannes Heinecke. Hyperbolic temporal knowledge graph embeddings with relational and time curvatures. In *ACL/IJCNLP (Findings)*, volume ACL/IJCNLP 2021 of *Findings of ACL*, pages 3296–3308, 2021.

[32] Chien-Chun Ni, Yu-Yao Lin, Feng Luo, and Jie Gao. Community detection on networks with ricci flow. *Scientific reports*, 9(1):1–12, 2019.

[33] Maximillian Nickel and Douwe Kiela. Poincaré embeddings for learning hierarchical representations. In *NeurIPS*, pages 6338–6347, 2017.

[34] Maximillian Nickel and Douwe Kiela. Learning continuous hierarchies in the lorentz model of hyperbolic geometry. In *ICML*, pages 3779–3788, 2018.

[35] Yann Ollivier. Ricci curvature of markov chains on metric spaces. *Journal of Functional Analysis*, 256(3): 810–864, 2009.

[36] Wei Peng, Jingang Shi, Zhaoqiang Xia, and Guoying Zhao. Mix dimension in poincaré geometry for 3d skeleton-based action recognition. In *ACM MM*, pages 1432–1440, 2020.

[37] Wei Peng, Tuomas Varanka, Abdelrahman Mostafa, Henglin Shi, and Guoying Zhao. Hyperbolic deep neural networks: A survey. *TPAMI*, 2021.

[38] Eric Qu and Dongmian Zou. Hyperbolic neural networks for molecular generation. *arXiv preprint arXiv:2201.12825*, 2022.

[39] Erzsébet Ravasz and Albert-László Barabási. Hierarchical organization in complex networks. *Physical review E*, 67(2):026112, 2003.

[40] Ramit Sawhney, Shivam Agarwal, Arnav Wadhwa, and Rajiv Shah. Exploring the scale-free nature of stock markets: Hyperbolic graph learning for algorithmic trading. In *WWW*, pages 11–22, 2021.

[41] Ryohei Shimizu, Yusuke Mukuta, and Tatsuya Harada. Hyperbolic neural networks++. In *ICLR*, 2020.

[42] Jianing Sun, Zhaoyue Cheng, Saba Zuberi, Felipe Pérez, and Maksims Volkovs. HGCF: Hyperbolic graph convolution networks for collaborative filtering. In *WWW*, pages 593–601, 2021.

[43] Li Sun, Zhongbao Zhang, Jiawei Zhang, Feiyang Wang, Hao Peng, Sen Su, and S Yu Philip. Hyperbolic variational graph neural network for modeling dynamic graphs. In *Proceedings of the AAAI Conference on Artificial Intelligence*, volume 35, pages 4375–4383, 2021.

[44] Li Sun, Zhongbao Zhang, Junda Ye, Hao Peng, Jiawei Zhang, Sen Su, and Philip S Yu. A self-supervised mixed-curvature graph neural network. *AAAI*, 2022.

[45] Zequn Sun, Muhao Chen, Wei Hu, Chengming Wang, Jian Dai, and Wei Zhang. Knowledge association with hyperbolic knowledge graph embeddings. *arXiv preprint arXiv:2010.02162*, 2020.

[46] Atsushi Suzuki, Atsushi Nitanda, Jing Wang, Linchuan Xu, Kenji Yamanishi, and Marc Cavazza. Generalization error bound for hyperbolic ordinal embedding. In *ICML*, pages 10011–10021, 2021.

[47] Atsushi Suzuki, Atsushi Nitanda, Linchuan Xu, Kenji Yamanishi, Marc Cavazza, et al. Generalization bounds for graph embedding using negative sampling: Linear vs hyperbolic. In *NeurIPS*, 2021.

[48] Yi Tay, Luu Anh Tuan, and Siu Cheung Hui. Hyperbolic representation learning for fast and efficient neural question answering. In *Proceedings of the Eleventh ACM International Conference on Web Search and Data Mining*, pages 583–591, 2018.

[49] Jake Topping, Francesco Di Giovanni, Benjamin Paul Chamberlain, Xiaowen Dong, and Michael M Bronstein. Understanding over-squashing and bottlenecks on graphs via curvature. In *ICLR*, 2022.

[50] Abraham A Ungar et al. The hyperbolic square and mobius transformations. *Banach Journal of Mathematical Analysis*, 1(1):101–116, 2007.

[51] Abraham Albert Ungar. A gyrovector space approach to hyperbolic geometry. *Synthesis Lectures on Mathematics and Statistics*, 1(1):1–194, 2008.

[52] Alexei Vázquez, Alessandro Flammini, Amos Maritan, and Alessandro Vespignani. Modeling of protein interaction networks. *Complexus*, 1(1):38–44, 2003.

[53] Petar Veličković, Guillem Cucurull, Arantxa Casanova, Adriana Romero, Pietro Lio, and Yoshua Bengio. Graph attention networks. *arXiv preprint arXiv:1710.10903*, 2017.

[54] Hao Wang, Defu Lian, Hanghang Tong, Qi Liu, Zhenya Huang, and Enhong Chen. Hypersorec: Exploiting hyperbolic user and item representations with multiple aspects for social-aware recommendation. *TOIS*, page 1–28, 2021.

[55] Liping Wang, Fenyu Hu, Shu Wu, and Liang Wang. Fully hyperbolic graph convolution network for recommendation. *arXiv preprint arXiv:2108.04607*, 2021.

[56] Quan Wang, Zhendong Mao, Bin Wang, and Li Guo. Knowledge graph embedding: A survey of approaches and applications. *TKDE*, 29(12):2724–2743, 2017.

[57] Shen Wang, Xiaokai Wei, Cicero Nogueira Dos Santos, Zhiguo Wang, Ramesh Nallapati, Andrew Arnold, and S Yu Philip. Knowledge graph representation via hierarchical hyperbolic neural graph embedding. In *IEEE Big Data*, pages 540–549. IEEE, 2021.

[58] Shen Wang, Xiaokai Wei, Cicero Nogueira Nogueira dos Santos, Zhiguo Wang, Ramesh Nallapati, Andrew Arnold, Bing Xiang, Philip S Yu, and Isabel F Cruz. Mixed-curvature multi-relational graph neural network for knowledge graph completion. In *WWW*, pages 1761–1771, 2021.

[59] Felix Wu, Amauri Souza, Tianyi Zhang, Christopher Fifty, Tao Yu, and Kilian Weinberger. Simplifying graph convolutional networks. In *ICML*, pages 6861–6871. PMLR, 2019.

[60] Zhenxing Wu, Dejun Jiang, Chang-Yu Hsieh, Guangyong Chen, Ben Liao, Dongsheng Cao, and Tingjun Hou. Hyperbolic relational graph convolution networks plus: a simple but highly efficient qsar-modeling method. *Briefings in Bioinformatics*, 22(5):bbab112, 2021.

[61] Keyulu Xu, Weihua Hu, Jure Leskovec, and Stefanie Jegelka. How powerful are graph neural networks? In *ICLR*, 2019.

[62] Menglin Yang, Ziqiao Meng, and Irwin King. Featurenorm: L2 feature normalization for dynamic graph embedding. In *ICDM*, pages 731–740, 2020.

[63] Menglin Yang, Min Zhou, Marcus Kalander, Zengfeng Huang, and Irwin King. Discrete-time temporal network embedding via implicit hierarchical learning in hyperbolic space. In *KDD*, pages 1975–1985, 2021.

[64] Menglin Yang, Zhihao Li, Min Zhou, Jiahong Liu, and Irwin King. Hicf: Hyperbolic informative collaborative filtering. In *Proceedings of the 28th ACM SIGKDD Conference on Knowledge Discovery and Data Mining*, pages 2212–2221, 2022.

[65] Menglin Yang, Min Zhou, Jiahong Liu, Defu Lian, and Irwin King. HRCF: Enhancing collaborative filtering via hyperbolic geometric regularization. In *WWW*, 2022.

[66] Menglin Yang, Min Zhou, Hui Xiong, and Irwin King. Hyperbolic temporal network embedding. *IEEE Transactions on Knowledge and Data Engineering*, 2022.

[67] Menglin Yang, Min Zhou, Lujia Pan, and Irwin King. κ hgcn: Tree-likeness modeling via continuous and discrete curvature learning. In *Proceedings of the 29th ACM SIGKDD Conference on Knowledge Discovery and Data Mining*, pages 2965–2977, 2023.

[68] Ke Yu, Shyam Visweswaran, and Kayhan Batmanghelich. Semi-supervised hierarchical drug embedding in hyperbolic space. *Journal of chemical information and modeling*, 60(12):5647–5657, 2020.

[69] Tao Yu and Christopher De Sa. Hyla: Hyperbolic laplacian features for graph learning. *arXiv preprint arXiv:2202.06854*, 2022.

[70] Hanqing Zeng, Hongkuan Zhou, Ajitesh Srivastava, Rajgopal Kannan, and Viktor Prasanna. GraphSAINT: Graph sampling based inductive learning method. In *ICLR*, 2020.

[71] Muhan Zhang and Yixin Chen. Link prediction based on graph neural networks. *NeurIPS*, 31, 2018.

[72] Sixiao Zhang, Hongxu Chen, Xiao Ming, Lizhen Cui, Hongzhi Yin, and Guandong Xu. Where are we in embedding spaces? a comprehensive analysis on network embedding approaches for recommender systems. In *KDD*, 2021.

[73] Yiding Zhang, Xiao Wang, Xunqiang Jiang, Chuan Shi, and Yanfang Ye. Hyperbolic graph attention network. *arXiv preprint arXiv:1912.03046*, 2019.

[74] Yiding Zhang, Xiao Wang, Chuan Shi, Xunqiang Jiang, and Yanfang Fanny Ye. Hyperbolic graph attention network. *TBD*, 2021.

[75] Yiding Zhang, Xiao Wang, Chuan Shi, Nian Liu, and Guojie Song. Lorentzian graph convolutional networks. In *WWW*, pages 1249–1261, 2021.

[76] Shichao Zhu, Shirui Pan, Chuan Zhou, Jia Wu, Yanan Cao, and Bin Wang. Graph geometry interaction learning. *NeurIPS*, 2020.

[77] Shichao Zhu, Shirui Pan, Chuan Zhou, Jia Wu, Yanan Cao, and Bin Wang. Graph geometry interaction learning. In *NeurIPS*, volume 33, pages 7548–7558, 2020.